

## ***EXOSAT* observations of a strong soft X-ray excess in MKN 841**

K. A. Arnaud,<sup>1</sup> G. Branduardi-Raymont,<sup>2</sup>  
 J. L. Culhane,<sup>2</sup> A. C. Fabian,<sup>1</sup> C. Hazard,<sup>3,1</sup>  
 T. A. McGlynn,<sup>1,4</sup> R. A. Shafer,<sup>1</sup> A. F. Tennant<sup>1</sup>  
 and M. J. Ward<sup>1</sup>

<sup>1</sup>*Institute of Astronomy, Madingley Road, Cambridge CB3 0HA*

<sup>2</sup>*Mullard Space Science Laboratory, University College London, Holmbury St Mary, Dorking, Surrey RH5 6NT*

<sup>3</sup>*Department of Physics and Astronomy, University of Pittsburgh, Pittsburgh, PA 15260, USA*

<sup>4</sup>*Space Telescope Science Institute, Homewood Campus, Baltimore, MD 21218, USA*

Accepted 1985 June 6. Received 1985 June 6; in original form 1985 April 29

**Summary.** *EXOSAT* observations of the spectrum of the Seyfert 1 galaxy MKN 841 show that it is well-fitted by a power law of photon index 1.6, similar to that of other Seyferts, and a large additional soft component. The X-ray luminosity over the observed band exceeds  $4 \times 10^{44}$  erg s<sup>-1</sup>. A single-temperature blackbody fit to the soft X-rays and the short-wavelength ultraviolet continuum gives a luminosity of  $2 \times 10^{46}$  erg s<sup>-1</sup> while an accretion disc spectrum fitted to the same points gives a luminosity of  $4.3 \times 10^{45}$  erg s<sup>-1</sup>. The flux measured by both the *EXOSAT* low- and medium-energy instruments exhibits 12 per cent amplitude variability on a time-scale of one day.

### **1 Introduction**

The Seyfert 1 galaxy MKN 841 is almost stellar in appearance and at a redshift of 0.0366. It lies in a field particularly well searched for QSOs at optical and radio wavelengths (Hazard & Sargent, in preparation) which was selected for a deep study using the Channel Multiplier Array (CMA) at the focus of the Low Energy Telescope (LE) of the European X-ray Observatory Satellite, *EXOSAT*. The image from the resulting 41-hour exposure with the thin Lexan filter is shown in Plate 1; MKN 841 was the only source detected. The Seyfert was bright in soft X-rays (as observed using the CMA with thin Lexan filter, which has a bandpass of 0.02–2.5 keV) and was also detected by the medium-energy collimated proportional counter (ME; with bandpass 1.5–15 keV). A description of the *EXOSAT* CMA detector can be found in de Korte *et al.* (1981) and of the ME detectors in Turner, Smith & Zimmerman (1981). The only previous report of X-ray emission from this source was by Halpern (1983) who gave *Einstein Observatory* MPC fluxes.

The X-ray spectrum that we obtain for MKN 841 provides clear evidence for a large excess of soft X-rays, well above the level predicted by extrapolating the ME spectrum into the LE energy band. In most Seyfert galaxies such an extrapolation is expected to fail at some low photon energy in order that the spectrum can rise to match the observed UV flux. However, the magnitude of the soft X-ray excess and the presence of a spectral turn-up at ultraviolet wavelengths in MKN 841 suggest that this connecting region contains a large 'bump' similar to, but much smaller than, that inferred for PG1211+143 by Elvis (1985). If this 'bump' is of blackbody shape (or a combination of blackbodies at different temperatures), then it dominates the luminosity of the source although the peak of the emission emerges in the unobservable XUV band. Whatever the precise spectral shape, MKN 841 is a very X-ray luminous Seyfert galaxy with  $L(0.15\text{--}15\text{ keV}) \approx 5 \times 10^{44} \text{ erg s}^{-1}$ . (We use  $H_0 = 50 \text{ km s}^{-1} \text{ Mpc}^{-1}$ .)

### The EXOSAT observations

A 42.2-hr exposure centred on  $\alpha = 15^{\text{h}} 00^{\text{m}} 48^{\text{s}}$ ,  $\delta = +10^{\circ} 48' 12''$  was made with EXOSAT on days 194 and 195 of 1984. The CMA with the thin Lexan filter was employed at the focus of the LE telescope for the last 41.2 hr after a 60-min exposure using the polypropylene filter. This filter has greater sensitivity to UV radiation than the Lexan filter and was used to confirm that any sources found were due to X-rays. No UV contamination sources were found. The image through the thin Lexan filter is shown in Plate 1.

A detailed statistical computer search on the raw image has revealed no other sources in the field, nor any evidence for the detection of the six QSOs brighter than 18 mag in the field (Table 1). This is not surprising given the low sensitivity of the LE CMA compared with that of the *Einstein Observatory* imaging instruments. It does, however, emphasize the remarkably high number (5) of serendipitous sources found in a much shorter CMA exposure of the Coma cluster by Branduardi-Raymont *et al.* (1985). The simplest explanation lies in a combination of a 'hole' in the absorbing matter within our galaxy along the line-of-sight in Coma and a steep soft-X-ray spectral gradient for AGNs (*cf.* Branduardi-Raymont *et al.* 1984 and Elvis 1985). Our lack of other sources shows that there is unlikely to be a 'hole' in the neutral hydrogen distribution in the vicinity of MKN 841. We therefore adopt a hydrogen column density of  $N_{\text{H}} = 2.9 \times 10^{20} \text{ atom cm}^{-2}$  for this region from the work of Stark *et al.* (in preparation) presented in Marshall & Clark (1984). Small angular size variations could make this value uncertain by up to  $\pm 1 \times 10^{20} \text{ atoms cm}^{-2}$  (M. Elvis, private communication). This will not substantially change any of our conclusions. In calculating the photoelectric absorption due to intervening matter we use the cross-sections and abundances of Morrison & McCammon (1983).

**Table 1.** X-ray upper limits for QSOs brighter than 18 mag in the field.

RA (h m s)	Dec ( $^{\circ}$ ' ")	Flux (0.15–2.0 keV) <sup>a</sup> $10^{-13} \text{ erg cm}^{-2} \text{ s}^{-1}$	Redshift <sup>b</sup>	B magnitude
15 02 03.5	+10 30 35	< 4.8	1.00	17.79
14 59 49.8	+10 16 49	< 6.6	0.93	17.78
15 00 40.5	+10 17 56	< 5.1	1.59	17.78
15 00 42.7	+10 16 05	< 5.4		17.39
15 02 17.2	+11 43 19	< 14.1	1.41	17.36
15 00 19.0	+11 27 43	< 9.9		17.65

Notes:

- $3\sigma$  upper limits have been calculated assuming a 1.6 photon index power-law and the same absorption as used for MKN 841 ( $N_{\text{H}} = 2.9 \times 10^{20} \text{ cm}^{-2}$ ).
- Redshifts given are from Hazard & Sargent (in preparation) as are the B magnitudes.

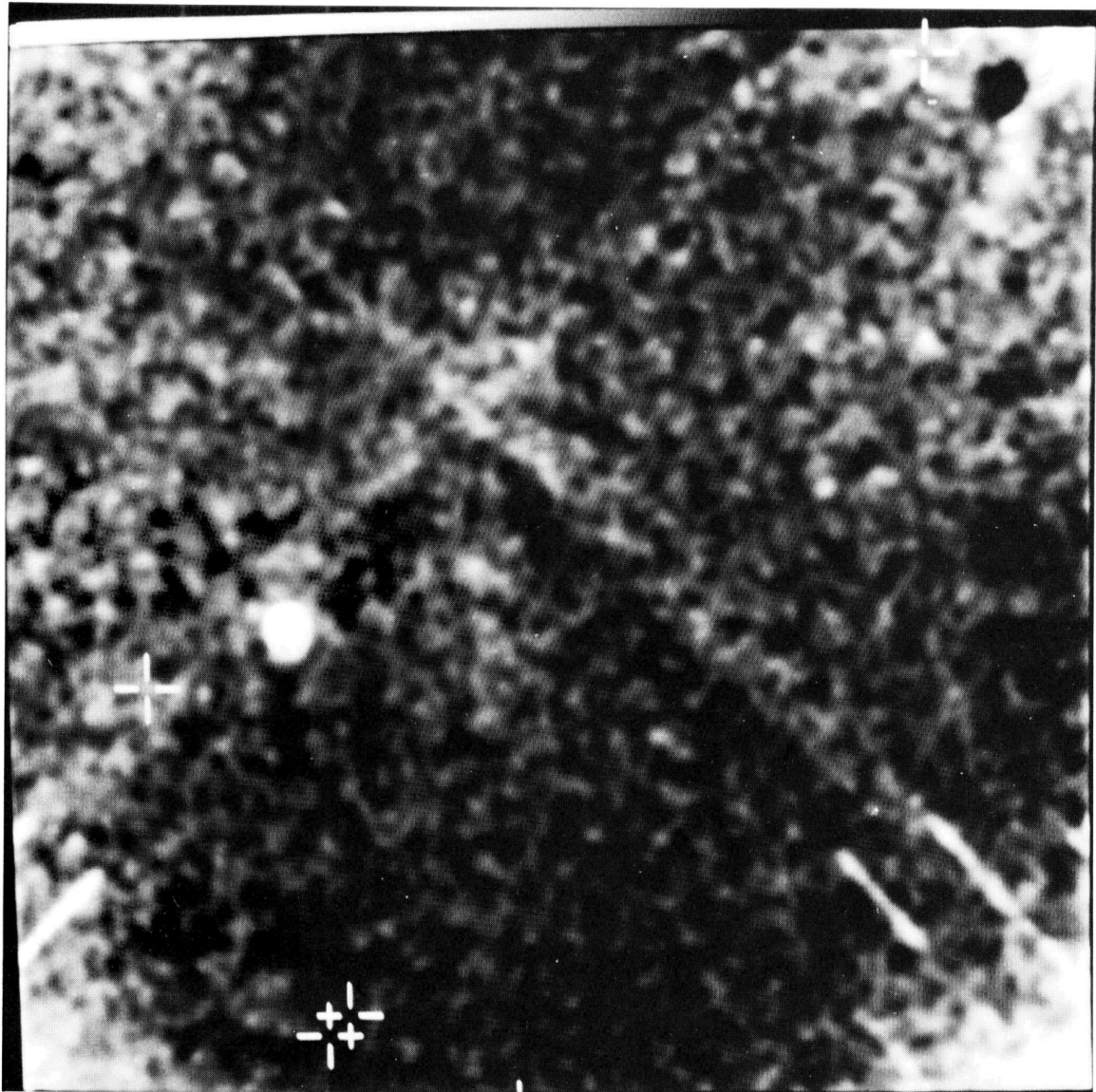


**Plate 1.** The central  $68 \times 68$  arcmin<sup>2</sup> of the EXOSAT CMA field. The grey scale is displayed on the right-hand edge of the image. The bottom (darkest) level corresponds to 3 and the top (brightest) level to 10 counts per  $8 \times 8$  arcsec<sup>2</sup> pixel. The image has been smoothed using a Gaussian with  $\sigma = 1$  arcmin. The white blob is MKN 841 and the exploded crosses indicate the positions of QSOs brighter than 18 mag from Hazard & Sargent (in preparation). The characteristic 'hotspot' in the middle of the CMA field has been removed during the analysis. It appears in one  $1/512$  s time bin every 128 s. The diagonal lines across the image are an electronic artefact. Several irregularities in the CMA are visible; the most obvious being the dark hole in the lower right-hand corner. [facing page 106]



MKN 841 was also detected by the ME instrument. The ME array comprises eight detectors each with a field of approximately 45 arcmin FWHM. The instrument is divided into two four-detector halves. The halves may be independently pointed at the target, or offset from the target by up to  $2^\circ$ . During this exposure one half was set pointing at the nominal target position,

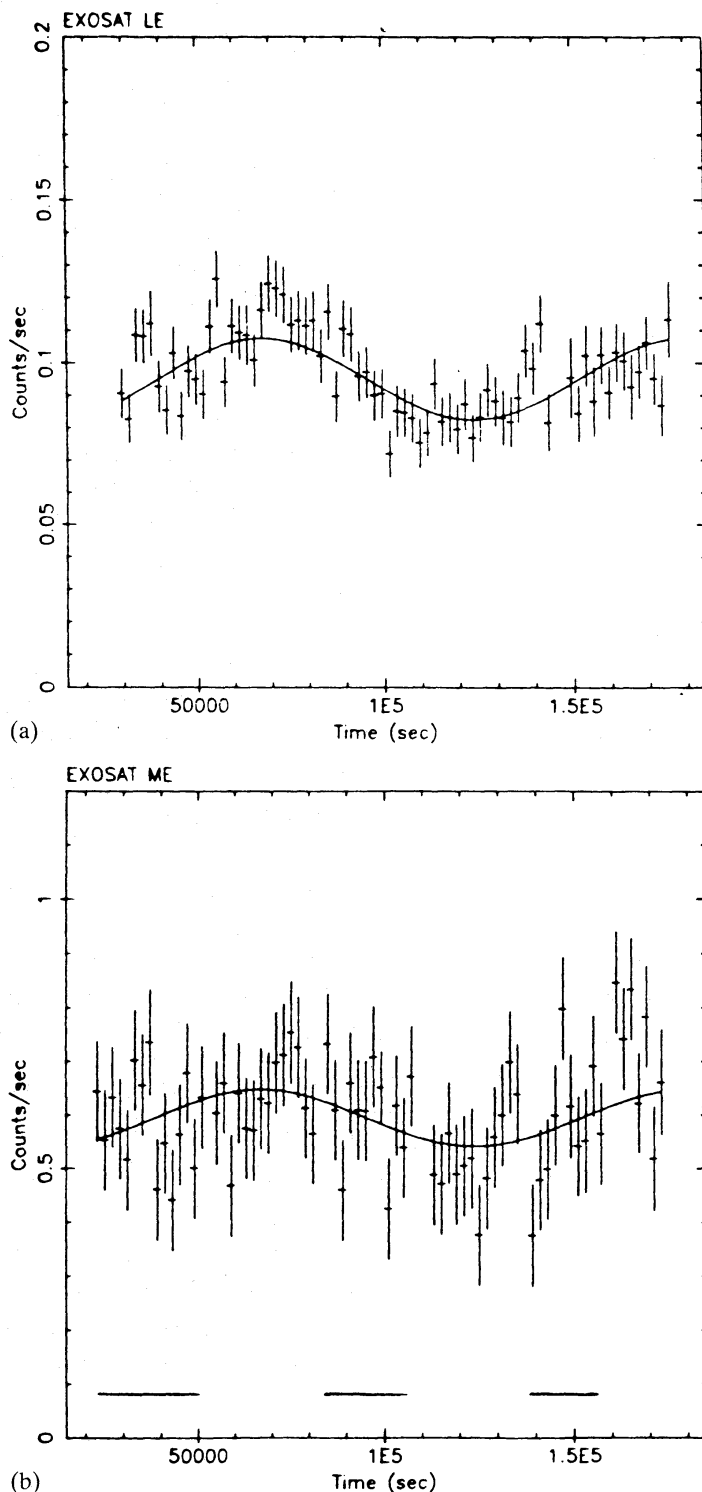


**Figure 1.** (a) LE and (b) ME X-ray light curves for MKN 841. Both light curves are in 2000-s bins and the model shown is the sine wave described in the text. The horizontal bars at the bottom of the ME plot show when the first half of the detector was on-source.

which included MKN 841 within the field of view, while the other half was offset to look at ‘blank’ sky. At intervals of approximately 30 000 s the halves were swapped so that reliable background measurements could be made for all detectors.

The X-ray light curve from the LE is shown in Fig. 1(a). The background has been subtracted from the LE data by using an off-source region in the image scaled to the same area as that of the source. The effective integration time was 132 000 s. The most obvious feature of the LE light curve is a slow oscillation in the count rate over the entire observation. We find that a simple sine wave plus a constant offset provides a reasonable fit to the data ( $\chi^2$  of 165.4 for 138 degrees of freedom). With this model the best-fitting period is  $111\,000 \pm 9000$  s with an amplitude of  $0.0125 \pm 0.0024$  count  $s^{-1}$  (90 per cent confidence). The quality of this fit suggests that there is no need to postulate variability on shorter time-scales, although indications of such variability are seen in Fig. 1(a). Note that our fit does not mean that the variability repeats in any regular manner as our observation is not long enough to tell. We have compared the source flux with the CMA temperature, high voltage level and background count rate and have found nothing which would cause the slow changes seen. Several short-term flares are seen in the background but these events do not appear in the source rate itself.

The ME light curve was constructed using data from channels 6 to 24 (out of a possible 1 to 128) of the argon detectors, a range of channels which gives a good signal-to-noise ratio. First the background was measured when each detector half was offset. The ME background is a weak function of the offset angle and the difference in the background between zero offset and the maximum offset is called the difference spectrum (Smith 1984). We used the standard difference spectrum to estimate the background level when the detector is aligned. For the selected channels the difference is small, being 0.01 count  $s^{-1}$  for half 1 and 0.04 count  $s^{-1}$  for half 2. Next we subtracted the estimated average background, assumed constant, from both the on-source half and the off-source half. This leaves source counts plus noise in the aligned half and just noise in the offset half. Since some of the noise is due to the changing radiation environment and should be roughly the same for both halves, we next subtracted the off-source half from the on-source half. This leaves a background subtracted rate that has been corrected for the known systematic effects seen in the ME.

The ME light curve is shown in Fig. 1(b). The effective on-source area is 525 cm<sup>2</sup>. The light curve is interesting in that there are indications of variability matching that seen in the LE. Fitting the ME data to a constant rate gives a  $\chi^2$  of 84.0 for 69 degrees of freedom. Adding a sine wave with the same period and phase as the best-fitting LE sine wave reduces  $\chi^2$  to 70.8 with a net loss of one degree of freedom. Using the F-statistic test, this reduction in  $\chi^2$  is significant at the greater than 99.8 per cent level. The best-fitting amplitude is  $0.060 \pm 0.028$  count  $s^{-1}$  which is 10 per cent of the mean rate. For the LE the amplitude was 13 per cent. We conclude that the LE sine wave model is a better fit to the ME rate than a constant. The correlation coefficient for the LE versus ME flux is 0.29 which has a less than 2 per cent probability of being due to chance. Thus from a statistical point of view, the model in which the ME shows variations in phase with the LE is preferred to a model in which the ME does not vary at all. As in the LE there is evidence for short-term variability. A few words of caution are necessary. The observed variability of the ME is very small and the error bars shown in Fig. 1(b) are calculated purely from Poisson statistics and do not include any systematics. Further, the inferred sinusoidal amplitude in the ME is much smaller than the observed background variability.

### 3 The X-ray spectrum of MKN 841

The count spectra of individual detectors of each half of the ME (four each) were corrected for the background using data collected from the offset pointings. As described in the previous section

there is a systematic difference between spectra taken with a detector pointed on-axis and the same detector offset (the difference spectrum). The inner pair of detectors in each half have by far the largest difference corrections, and are therefore more prone to systematic errors. For this reason we have not included them in the subsequent analysis. We note, however, that the rejected count spectra are consistent with the results derived below, although with a larger region of allowed parameters.

The remaining count spectra were fitted simultaneously with the same model spectrum, which was characterized by a power-law of photon index  $\Gamma$  absorbed by a line-of-sight column density,  $N_{\text{H}}$ . The best-fitting spectrum gave a  $\chi^2$  of 304.95 (for 285 degrees of freedom) for  $\Gamma=1.59$ . This result is relatively insensitive to  $N_{\text{H}}$  unless it exceeds  $10^{21} \text{ cm}^{-2}$  (Fig. 2).  $\Gamma$  lies between 1.3 and 1.9 (with 99.9 per cent confidence) and agrees well with typical values determined elsewhere for brighter Seyfert 1 galaxies in the range 0.75–10 keV (Mushotzky 1982; Petre *et al.* 1984).

We then extrapolated single power-law models which fit the ME spectrum to lower energies in order to predict the LE flux (fixing  $N_{\text{H}}=2.9 \times 10^{20} \text{ cm}^{-2}$ ; Fig. 3). The observed LE flux is 5.7 times the ME best-fit prediction with a 90 per cent lower limit of 4.0 times the prediction. We have therefore investigated a two-component power-law model by introducing a further soft slope  $\Gamma_{\text{S}}$ . With 99 per cent confidence, we find that  $\Gamma_{\text{S}} > 2.8$  if  $N_{\text{H}}$  exceeds  $2.9 \times 10^{20} \text{ cm}^{-2}$  (Fig. 4) (where we have constrained  $\Gamma$  within the range 1.3 to 1.9).  $\Gamma_{\text{S}}$  only drops below 1.9, and is then compatible with a single power-law, if  $N_{\text{H}} \leq 4 \times 10^{19} \text{ cm}^{-2}$ . This is far too low to be acceptable (*cf.* Section 2) and we conclude that MKN 841 shows a strong soft X-ray excess flux. We note that  $\Gamma_{\text{S}}$  is largely determined by our one LE point with the ME data constraining the cross-over point of the two power-laws to lie below  $\sim 1$  keV. Inclusion of the 60 min of polypropylene data argues for a still steeper index ( $\Gamma_{\text{S}} \geq 7.5$ ). Note that a slight ( $\sim 20$  per cent) variation of the source intensity could also explain the higher polypropylene count rate.

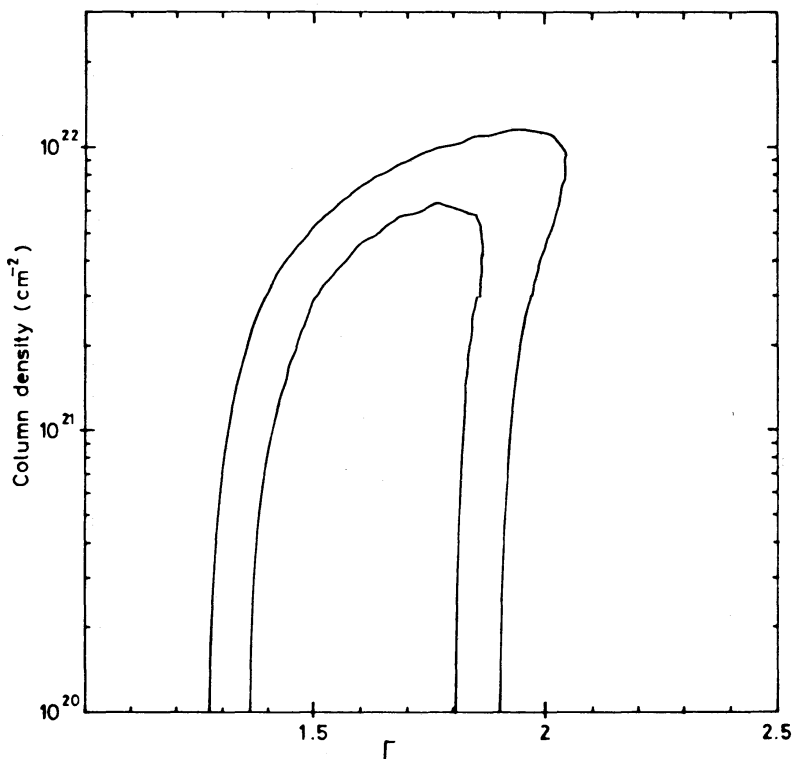
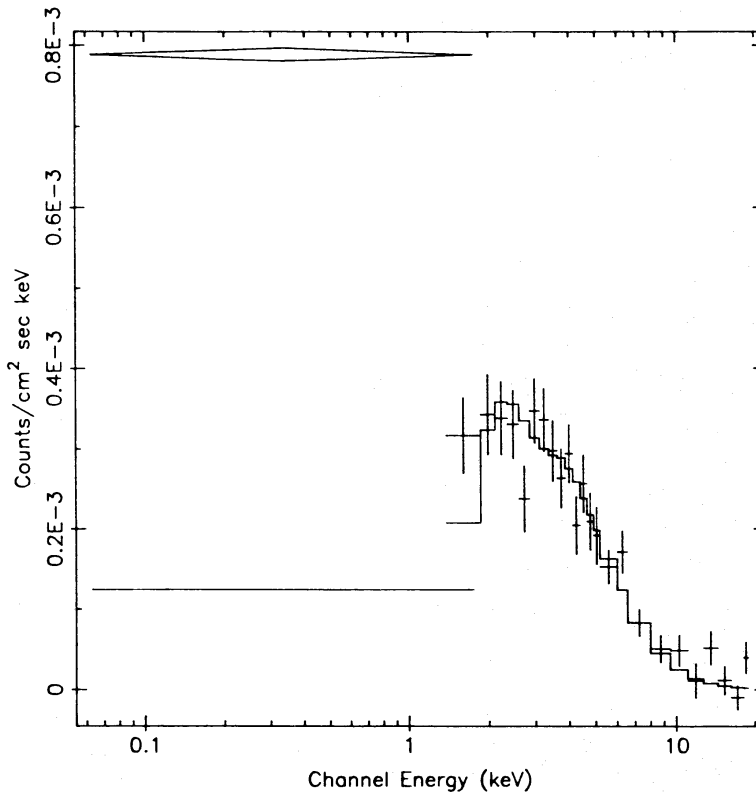
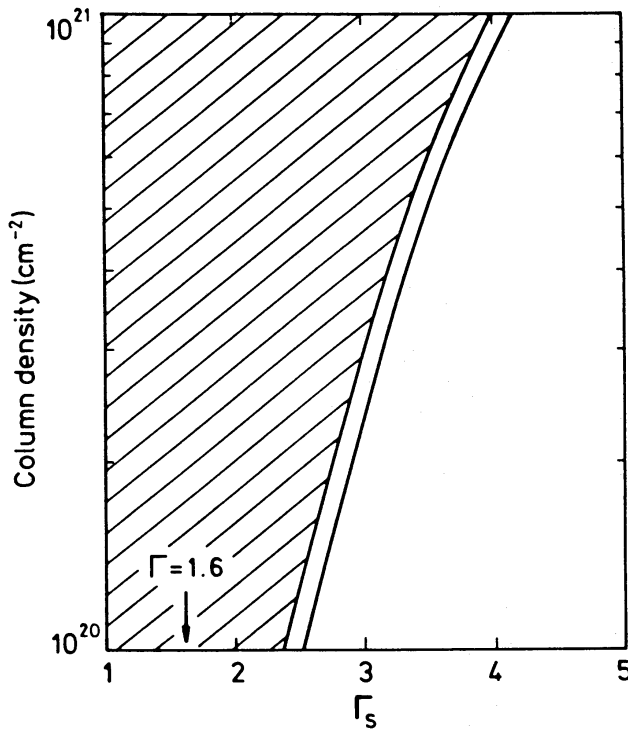


Figure 2.  $\chi^2$  contours of photon power-law index against absorption for fits to the ME data. Contours are the 90 and 99 per cent confidence levels for two interesting parameters.



**Figure 3.** Combined LE and ME spectrum for MKN 841. The crosses are the ME data points and the diamond is the LE thin Lexan measurement. The model (continuous line) has been folded through the instrumental response and is the best fit to the ME data. The horizontal line is the LE flux predicted by the ME model.



**Figure 4.**  $\chi^2$  contours of photon power-law index  $\Gamma_s$  for the soft component against absorption for fits to the LE and ME data. Contours are 90 and 99 per cent confidence levels for two interesting parameters and the hatched region indicates values of the soft power-law index outside the 99 per cent confidence region. The LE datum may contain a further systematic uncertainty of up to 10 per cent (P. Giommi, private communication). This would require  $N_H < 8 \times 10^{19} \text{ cm}^{-2}$  for an acceptable power-law fit.



The 2–10 keV flux from MKN 841 is  $1.58 \times 10^{-11} \text{ erg cm}^{-2} \text{ s}^{-1}$  (with  $1\text{-}\sigma$  errors of 4.9 per cent) leading to an X-ray luminosity,  $L_X = 8.4 \times 10^{43} \text{ erg s}^{-1}$ . Halpern (1983) found  $L_X$  (2–10 keV) =  $1.2 \times 10^{44} \text{ erg s}^{-1}$  and  $4.7 \times 10^{43} \text{ erg s}^{-1}$  at the beginning and end of 1980. The absorption-corrected X-ray flux between 0.15 (below which absorption causes the spectrum to drop dramatically) and 2 keV is  $6.7 \times 10^{-11} \text{ erg cm}^{-2} \text{ s}^{-1}$ , leading to  $L_X$  (0.15–2 keV) =  $2.7 \times 10^{44} \text{ erg s}^{-1}$ , and  $L_X$  (0.15–20 keV) =  $4.2 \times 10^{44} \text{ erg s}^{-1}$  for the two power-law model used above.

#### 4 The overall spectral distribution of MKN 841

The energy distribution of MKN 841 from  $100 \mu\text{m}$  to 20 keV is shown in Fig. 5 (from Ward *et al.* 1985 and references therein). The near-to mid-infrared spectrum is close to a power law of energy index  $1.25 \pm 0.12$  as is often found in Seyfert 1 galaxies (Ward *et al.* 1985). The continuum flattens sharply from 25 to  $60 \mu\text{m}$ , turning over toward the radio band where MKN 841 emits a few mJy at 1415 MHz. The integrated infrared luminosity is  $L_{\text{IR}}(2\text{--}20 \mu\text{m}) = 4.4 \times 10^{44} \text{ erg s}^{-1}$ . Below  $1 \mu\text{m}$  the continuum flattens and then rises to a strong Balmer continuum and blended Fe II emission ‘bump’ centred around  $\sim 3800 \text{ \AA}$ . At the shortest observable wavelengths in the ultraviolet ( $< 1500 \text{ \AA}$  from the *IUE*), the spectrum is rising and gives the appearance of a turn-up. The *IUE* fluxes were obtained by measurement of microfiche plots (Rutherford Appleton Laboratory 1984).

We have fitted the X-ray spectrum with a two-component model composed of a blackbody and a power law. The blackbody has been constrained to pass through the (dereddened) shortest

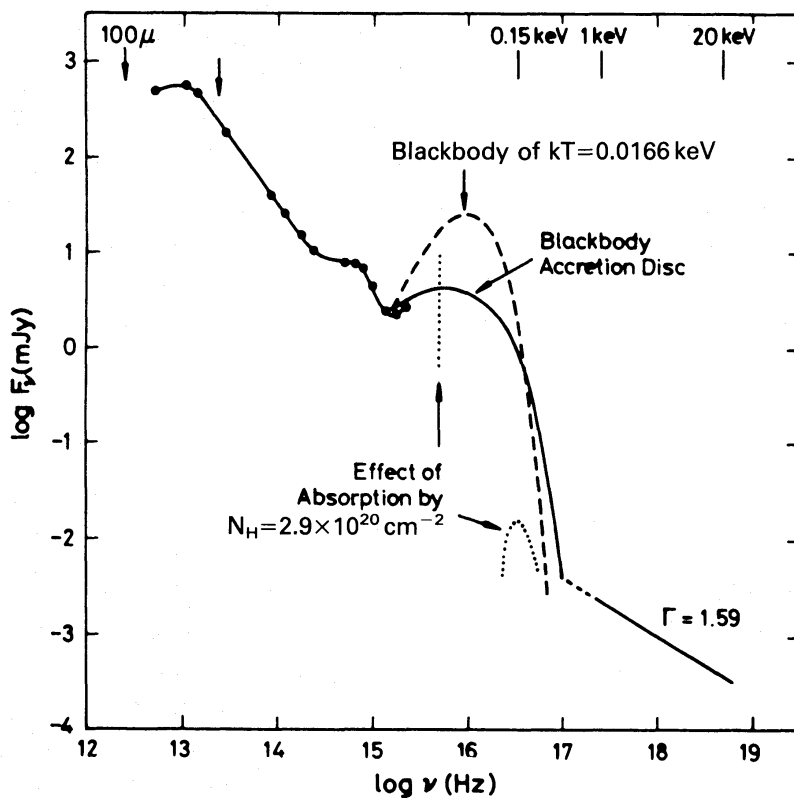


**Figure 5.** The overall spectral distribution of MKN 841 from the infrared to the hard X-ray. The infrared to UV points are from Ward *et al.*; the far-infrared upper limits (marked by arrows) are from *IRAS* and the UV points are from *IUE*. The hard X-ray slope is from the *EXOSAT* ME data. The UV has been joined by the hard X-ray with two illustrative spectra: a single-temperature blackbody (dashed) and a blackbody accretion disc (full line). The dotted lines show the blackbody spectrum after Galactic absorption has been taken into account.

wavelength UV datum (3 mJy at 1500 Å). Our best-fitting blackbody is the dashed line in Fig. 5 and has a temperature corresponding to  $kT_{\text{bb}}=0.0166$  keV, or  $T=200\,000$  K, and a total luminosity of  $2.2\times 10^{46}$  erg s<sup>-1</sup>. Uncertainties in the UV flux lead to uncertainties in this luminosity of  $\pm 50$  per cent. The emitting area is  $1.8\times 10^{29}$  cm<sup>2</sup>, corresponding to the surface of a sphere of radius  $1.2\times 10^{14}$  cm; this is a few Schwarzschild radii ( $R_s$ ) of a  $10^8 M_\odot$  black hole, for which  $\sim 2\times 10^{46}$  erg s<sup>-1</sup> is the Eddington luminosity.

For comparison, we have also fitted the spectrum of a face-on blackbody accretion disc (see e.g. Pringle 1981), shown as a thin line in Fig. 5. The total luminosity of that component,  $L_d$ , is  $4.3\times 10^{45}$  erg s<sup>-1</sup>. Identifying the inner radius of the disc with the innermost stable orbit about a central (non-rotating) black hole, the characteristic temperature of the disc,  $T_*$ , of  $7.0\times 10^5$  K and  $L_d$  determine a mass for the hole of  $8\times 10^6 M_\odot$  and an accretion rate of  $0.9 M_\odot \text{ yr}^{-1}$  (with an efficiency of 1/12). The total luminosity inferred is then inconsistent with the Eddington limit of  $1.6\times 10^{45}$  erg s<sup>-1</sup> for such a mass. (Reasonable uncertainties in the values of  $N_H$  and dereddening of the UV continuum do not change this result by more than a factor of 2.) It is, however, unlikely that the innermost regions of the source are in thermodynamic equilibrium. An inner disc will not radiate then as a true blackbody and in order to emit the same luminosity the disc temperature must increase and the value of  $T_*$  estimated from the data will be too high. The inferred black-hole mass depends inversely upon this estimate of  $T_*$  so the mass derived above is a lower limit. If, for example, the mass is  $2\times 10^8 M_\odot$ , then the  $10^5$  s variability that we observe is comparable with the Keplerian orbital period of matter at  $\sim 10 R_s$ .

The peak-to-trough time-scale (maximum to minimum flux) of our sinusoidal fit is  $56\,000\pm 4\,000$  s which is about half a day. Previous observations (Zamorani *et al.* 1984; Tennant & Mushotzky 1983; Pounds 1979) of X-ray variability from other active galaxies have shown that a one-day time-scale is often seen. It is interesting that both the hard power-law and soft-excess components seem to vary with a similar relative amplitude and phase. This presumably indicates a close relationship between them. The maximum rate of change of the LE luminosity is  $9\times 10^{36}$  erg s<sup>-2</sup> over the observed band. This implies that the efficiency of converting matter into radiation must then exceed 0.04 per cent (Fabian 1979). If the blackbody model with  $L_{\text{bb}}=2\times 10^{46}$  erg s<sup>-1</sup> is appropriate then the source converts matter to energy with an efficiency  $>2$  per cent. This limit is obtained by assuming that only electron scattering is important and that the optical depth is 1. A blackbody (or even a Wien peak) necessarily demands greater opacity. The wider implications of a strong source of EUV/XUV radiation in a Seyfert 1 galaxy are discussed elsewhere.

## 5 Conclusions

The Seyfert 1 galaxy MKN 841 is a strong source of soft X-rays with a luminosity in the energy range 0.15–15 keV of at least  $4\times 10^{44}$  erg s<sup>-1</sup>. No other objects in the CMA field were detected in an exposure of 42 hr. The 2–10 keV spectrum of MKN 841 is a power law of photon index 1.6, similar to that of other Seyfert 1 galaxies. The strong soft X-ray emission must be due to another spectral component. This, together with a turn-up in the continuum spectrum at the shortest ultraviolet wavelengths, suggests the presence of a large flux in the extreme ultraviolet. Both the soft and power-law components of MKN 841 vary with an amplitude of  $\sim 12$  per cent on a time-scale of 1 day. It is important to seek confirmation of the presence of the large extreme ultraviolet flux by, for example, looking for correlated UV and X-ray variability.

## Acknowledgments

We thank the *EXOSAT* Observatory staff for their assistance during the observation and in answering subsequent queries. ACF thanks the Royal Society for support.

## References

- Branduardi-Raymont, G., Bell-Burnell, J., Kellett, B., Fink, H., Molteni, D. & McHardy, I., 1984. In: *Advances in Space Research*, Pergamon Press, Oxford.
- Branduardi-Raymont, G., Mason, K. O., Murdin, P. G., Martin, C. & McKechnie, S. P., 1985. Preprint.
- de Korte, P. A. J., Bleeker, J. A. M., den Boggende, A. J. F., Branduardi-Raymont, G., Brinkman, A. C., Culhane, J. L., Gronenschild, E. H. B. M., Mason, I. & McKechnie, S. P., 1981. *Space Sci. Rev.*, **30**, 495.
- Elvis, M., 1985. Preprint.
- Fabian, A. C., 1979. *Proc. R. Soc. Lond. A*, **366**, 449.
- Halpern, J., 1983. *PhD thesis*, Harvard University.
- Marshall, F. J. & Clark, G. W., 1984. *Astrophys. J.*, **287**, 633.
- Morrison, R. & McCammon, D., 1983. *Astrophys. J.*, **270**, 119.
- Mushotzky, R. F., 1982. *Astrophys. J.*, **256**, 92.
- Petre, R., Mushotzky, R. F., Krolik, J. K. & Holt, S. S., 1984. *Astrophys. J.*, **280**, 499.
- Pounds, K. A., 1979. *Proc. R. Soc. Lond. A*, **366**, 375.
- Pringle, J. E., 1981. *Ann. Rev. Astr. Astrophys.*, **19**, 137.
- Smith, A., 1984. *EXOSAT Express*, **5**, 48.
- Tennant, A. F. & Mushotzky, R. F., 1983. *Astrophys. J.*, **264**, 92.
- Turner, M. J. L., Smith, A. & Zimmerman, H. U., 1981. *Space Sci. Rev.*, **30**, 479.
- Ward, M. J., Elvis, M., Fabbiano, G., Carleton, N., Willner, S. P. & Lawrence, A., 1985. Preprint.
- Zamorani, G., Giommi, P., Maccacaro, T. & Tananbaum, H., 1984. *Astrophys. J.*, **278**, 28.